

Comparison of Different hp - Adaptive Strategies in Viscoelastic Flow Simulation

V. Warichet*

V. Legat*

Abstract

Accurate and stable numerical methods are particularly important in viscoelastic flow simulations. Local h - and p -refinements are introduced in order to obtain very high rates of convergence, even in the presence of singularities. We present several adaptive strategies, based on an error estimator which is an extension of some rigorous results of Oden, Wu and Ainsworth ([13, 1, 2]). For Navier-Stokes equations, error estimation and adaptivity have already been exploited in [14]. Numerical results obtained illustrate both the validity of the error estimation technique and the efficiency of the adaptive procedure chosen. A comparison is made for each problem between different adaptive strategies.

Key words: hp -finite element, error estimation, viscoelastic flows, boundary discontinuities.

AMS subject classifications: 65N15, 65N30, 65N50, 76A10.

1 Introduction

Accurate and stable numerical methods are particularly important in viscoelastic flow simulations. More and more attention has been devoted to spectral ([4], [9], [16]) and high order methods ([17]). For smooth problems, those methods exhibit an exponential rate of convergence and an improved robustness when increasing the elasticity of the fluid. In order to extend these properties to practical applications with singularities, we describe an hp -adaptive finite element method. The particular choice of hierarchical shape functions and the use of 1-irregular meshes allow

*CESAME, Université Catholique de Louvain, 4 avenue G. Lemaitre, B-1348, Louvain-la-Neuve, Belgium

ICOSAHOM'95: Proceedings of the Third International Conference on Spectral and High Order Methods. ©1996 Houston Journal of Mathematics, University of Houston.

us to introduce an interesting combination of local h - and p -refinements ([8]).

The element size h and the order of approximation p are adjusted by different adaptive strategies in order to obtain very high rates of convergence, even in the presence of singularities. Our strategies, based on *a priori* and *a posteriori* error estimates, produce hp -finite element meshes, so that the computer time required to achieve a target error is significantly reduced.

Numerical results obtained with the classical Upper Convected Maxwell-B (UCM) fluid and the Modified Upper Convected Maxwell (MUCM) fluid illustrate both the validity of the error estimation technique and the efficiency of the adaptive procedure chosen. A comparison is made for each problem between different adaptive strategies.

2 Governing equations

We consider the steady flow of an incompressible viscoelastic fluid in a domain Ω . If we neglect inertia, the conservation equations are :

$$(1) \quad \begin{aligned} -\nabla \cdot \boldsymbol{\sigma} &= \mathbf{f} \\ \nabla \cdot \mathbf{u} &= 0 \end{aligned}$$

where \mathbf{u} is the velocity field, \mathbf{f} the body force, $\boldsymbol{\sigma}$ the Cauchy stress tensor.

On the other hand, the MUCM constitutive equations (see [3, 5]), describing the viscoelastic properties of the fluid, are the following:

$$(2) \quad \begin{aligned} \boldsymbol{\sigma} &= \boldsymbol{\tau}_N + \boldsymbol{\tau}_V - p\mathbf{I} \\ \boldsymbol{\tau}_N &= 2\eta_N \mathbf{D}(\mathbf{u}) \\ \boldsymbol{\tau}_V + \lambda(\text{tr}(\boldsymbol{\tau}_V)) \overset{\nabla}{\boldsymbol{\tau}}_V &= 2\eta_V \mathbf{D}(\mathbf{u}) \end{aligned}$$

where p is the pressure, \mathbf{I} the unit tensor, $\mathbf{D}(\mathbf{u})$ is the strain rate tensor.

The Cauchy stress tensor is splitted into a Newtonian component $\boldsymbol{\tau}_N$ and a viscoelastic contribution $\boldsymbol{\tau}_V$. η_N and η_V are the associated dynamic viscosities. The symbol

∇ denotes the upper convected derivative and λ is the relaxation time of the fluid, defined as follows :

$$(3) \quad \lambda(\text{tr}(\boldsymbol{\tau}_V)) = \frac{\lambda_0}{1 + \left(\frac{\text{tr}(\boldsymbol{\tau}_V)F(\lambda_0\dot{\gamma}_0)}{\eta_V\dot{\gamma}_0} \right)^{\alpha-1}}$$

where $\dot{\gamma}_0$ is a characteristic shear rate of the problem.

Dirichlet boundary conditions are imposed on velocities at inflow sections and along rigid walls ($\partial\Omega_D$) while extra-stresses are imposed at inflow sections $\partial\Omega_{Inflow}$ only. Dirichlet and classical Robin conditions are imposed on the velocity field respectively at outflow sections $\partial\Omega_{Outflow} \subset \partial\Omega_D$ and along axis of symmetry $\partial\Omega_R$.

Remark 1 Unlike classical Oldroyd-B model ($F = 0$) or Maxwell-B model ($\eta_N = 0$; $F = 0$), the MUCM model guarantees the well-posedness ([5]) of the boundary value problem, as the stresses $\boldsymbol{\tau}_V$ remain square integrable at geometrical singularities.

The problem can be characterized by the *Weissenberg* number which compares elastic and viscous forces in the fluid. Taking V as a typical velocity and R as a typical length of the problem, it is defined as :

$$We = \lambda V/R,$$

A weak formulation of (1),(2),(3) is built using a weighted residual method. The components of the solution vector $(\boldsymbol{\tau}_V, \mathbf{u}, p)$ are chosen inside the following spaces:

$$\begin{aligned} S &= \{ \boldsymbol{\tau}_V \in (H^1(\Omega))^m : \boldsymbol{\tau}_V = \hat{\boldsymbol{\tau}}_V \text{ on } \partial\Omega_{Inflow} \} \\ V &= \{ \mathbf{u} \in (H^1(\Omega))^n : \mathbf{u} = \hat{\mathbf{u}} \text{ on } \partial\Omega_D, \mathbf{u} \cdot \mathbf{n} = 0 \text{ on } \partial\Omega_R \} \\ Q &= \{ p \in L^2(\Omega) : \int_{\Omega} p dx = 0 \} \end{aligned}$$

3 Spatial discretization of the problem

We select a suitable finite dimensional subspace $T^{hp}(\Omega)$ inside $S \times V \times Q$ ¹ and rewrite the discrete form of the weak problem using the classical Galerkin's method.

Given body forces $\mathbf{f} \in V^*$, find $(\boldsymbol{\tau}_V^{hp}, \mathbf{u}^{hp}, p^{hp}) \in T^{hp}(\Omega)$ such that

$$(4) \quad \int_{\Omega} (\boldsymbol{\tau}_V^{hp} \cdot \mathbf{s} + \lambda \boldsymbol{\tau}_V^{hp} \cdot \mathbf{s}) dx = \int_{\Omega} 2\eta_V \mathbf{D}(\mathbf{u}^{hp}) \cdot \mathbf{s} dx$$

$$(5) \quad \int_{\Omega} (\boldsymbol{\sigma} : \mathbf{D}(\mathbf{v}) - \mathbf{f} \cdot \mathbf{v}) dx = 0$$

$$(6) \quad \int_{\Omega} q \nabla \cdot \mathbf{u}^{hp} dx = 0$$

¹A detailed description of $T^{hp}(\Omega)$ is given in [18]

$$\forall (\mathbf{s}, \mathbf{v}, q) \in T^{hp}(\Omega)$$

$T^{hp}(\Omega)$ is built in order to keep the discrete solution in $C^0(\bar{\Omega})$ when local refinements are applied. At the elemental level, the solution is approximated using hierarchical shape functions. The orders of approximation associated with each field cannot be chosen independently. We use the Ladyzhenskaya-Brezzi-Babuška (LBB) condition to select the pressure approximation and, from numerical experiments presented in [18], we take $p_{velocity} = p_{extra-stress} - 1$. As in [8], we restrict ourselves to 1-irregular meshes. Additional constraints are imposed along irregular interfaces in order to enforce the C^0 -continuity. Local p -refinement of an element doesn't involve any additional constraints. Its neighbours are automatically enriched by the addition of extra shape functions.

The whole system is solved by a fully coupled Newton-Raphson scheme and a direct solver.

4 Adaptive strategy

First, we recall briefly our adaptive strategy which is a generalized version of the procedure given in [12] and exploited in [10].

4.1 A priori error estimation

From the definition of the approximation space $T^{hp}(\Omega)$, the following local interpolation property holds for each scalar variable on element $\Omega_K (1 \leq K \leq N^h)$:

$$(7) \quad \|u - \tilde{u}^{hp}\|_{s, \Omega_K} \leq C \frac{h_K^{\min(p_K+1-s, r-s)}}{p_K^{r-s}} \|u\|_{r, \Omega_K}$$

where $u \in H^r(\Omega)$, $r > s$, \tilde{u}^{hp} is an appropriate approximation of u , $\| \cdot \|_{s, \Omega_K}$ is an usual Sobolev norm, h_K is the maximal diagonal length inside Ω_K and p_K is the lowest order of approximation of \tilde{u}^{hp} inside Ω_K .

As a well-known property in all viscoelastic flows, we expect the extra-stresses to be mainly affected by errors. The convective term in the constitutive equations (2), stress concentration near geometrical singularities and the appearance of very thin stress boundary layers due to the presence of normal stresses are the three main reasons for inaccuracies in viscoelastic flow simulation (see [6]).

To extend the interpolation error (7) to our multivariable problem, an energy-like norm is defined on $S \times V \times Q$ as the sum of the following quantities:

$$\|(\mathbf{s}, \mathbf{v}, q)\|_K^2 = \sum_{K=1}^{N^h} \int_{\Omega_K} \mathbf{s} \cdot \mathbf{s} + 2\eta_N \mathbf{D}(\mathbf{v}) : \mathbf{D}(\mathbf{v}) + q^2 dx$$

An *a priori* error estimator is therefore available by rewriting Equation (7) :

$$(8) \quad |||(\boldsymbol{\tau}^{error}, \mathbf{u}^{error}, p^{error})|||_K^2 \leq \frac{h_K^{2\mu_K}}{p_K^{2\nu_K}} \Lambda_K^2$$

where Λ_K , μ_K , ν_K are local unknown constants and the reference order of approximation p_K is taken from the stress field interpolation.

We assume that the actual error $|||(\boldsymbol{\tau}^{error}, \mathbf{u}^{error}, p^{error})|||_K$ in Equation (8) is available to sufficient accuracy through an *a posteriori* error estimator.

4.2 A posteriori error estimation

We use an error residual method developed in [11, 13, 1, 2]. We generalize here this approach for viscoelastic flows.

The global *a posteriori* error estimate θ_i for a given mesh \mathcal{P}_i is defined as follows

$$\theta_i = \sqrt{\sum_{K=1}^N \theta_{i,K}^2}$$

where $\theta_{i,K}$ is the local error estimator computed on each element Ω_K . We have :

$\theta_{i,K} = |||(\boldsymbol{\tau}_K^{est}, \mathbf{u}_K^{est}, p_K^{est})|||_K$
where $(\boldsymbol{\tau}_K^{est}, \mathbf{u}_K^{est}, p_K^{est}) \in S_K \times V_K \times Q_K$ is such that

$$(9) \quad \int_{\Omega_K} \boldsymbol{\tau}_K^{est} \cdot \mathbf{s}_K dx = \int_{\Omega_K} (\boldsymbol{\tau}_K^{hp} \cdot \mathbf{s}_K + \lambda \boldsymbol{\tau}_K^{hp} \cdot \nabla \mathbf{s}_K) dx - \int_{\Omega_K} 2\eta_V \mathbf{D}(\mathbf{u}_K^{hp}) \cdot \mathbf{s}_K dx$$

$$(10) \quad \int_{\Omega_K} 2\eta_N \mathbf{D}(\mathbf{u}_K^{est}) : \mathbf{D}(\mathbf{v}_K) dx = \int_{\Omega_K} -\boldsymbol{\sigma}_K(\boldsymbol{\tau}_K^{hp}, \mathbf{u}_K^{hp}, p_K^{hp}) : \mathbf{D}(\mathbf{v}_K) dx + \int_{\partial\Omega_K} \langle \mathbf{n}_K \cdot \boldsymbol{\sigma}^{est}(\boldsymbol{\tau}_K^{hp}, \mathbf{u}_K^{hp}, p_K^{hp}) \rangle \cdot \mathbf{v}_K ds + \int_{\Omega_K} \mathbf{f} \cdot \mathbf{v}_K dx$$

$$(11) \quad \int_{\Omega_K} p_K^{est} q_K dx = \int_{\Omega_K} q_K \nabla \cdot \mathbf{u}_K^{hp} dx$$

$$\forall \mathbf{s}_K \in S_K, \forall \mathbf{v}_K \in V_K, \forall q_K \in Q_K, 1 \leq K \leq N^h.$$

where S_K , V_K and Q_K are the restrictions of S , V and Q to element Ω_K and $\langle \mathbf{n}_K \cdot \boldsymbol{\sigma}^{est}(\boldsymbol{\tau}_K^{hp}, \mathbf{u}_K^{hp}, p_K^{hp}) \rangle$ is a flux term appearing in the local problem, as the continuity constraints have been relaxed at the interelement boundaries.

Remark 2 Note that $\boldsymbol{\tau}_K^{est}$ and p_K^{est} are obtained straightforwardly from Equations (9) and (11), while a small Poisson problem is required to find \mathbf{u}_K^{est} .

4.3 Adaptive strategy

Let us start with an initial mesh \mathcal{P}_i ($i = 0$), where we solve an *hp*-discrete problem and we compute the *a posteriori* error estimator $\theta_{i,K}$ on each element Ω_K . A new mesh \mathcal{P}_{i+1} is obtained by means of local *h*-refinements or *p*-enrichments in order to reach a given level of accuracy θ^{tgt} . Such modifications of both mesh size distribution and polynomial degree distribution are derived by taking advantage of the *a priori* and the calculated *a posteriori* error estimates. If pure *h*-refinements are applied, the number n_K of new subelements inside each element of \mathcal{P}_i has to satisfy

$$(12) \quad n_K = \left[N_{i+1}^h \frac{(\theta_{i,K})^2}{(\theta^{tgt})^2} \right]^{\frac{1}{\mu}}$$

$$(13) \quad N_{i+1}^h = \sum_{K=1}^{N_i^h} n_K$$

A description of the pure *p*-refinements needed to reach a prescribed level θ^{tgt} is obtained from the following expression.

$$(14) \quad p_{i+1,K} = \left[N_i^h \frac{(\theta_{i,K})^2}{(\theta^{tgt})^2} (p_{i,K})^{2\nu} \right]^{\frac{1}{2\nu}}$$

Remark 3 Several numerical experiments have shown that abrupt increase of the order of approximation between two neighbouring elements can be detrimental for the accuracy of the solution. We will therefore prevent these jumps in the *p*-distribution by adding extra-elements to the list given by Equation (14).

We now apply our method to two model problems : the flow around a sphere falling in a cylinder and the flow in an axisymmetric contraction.

5 Numerical results

The first implementation of *hp*-finite element methods was developed at TICAM by Demkowicz and Oden over a 7-year period [8, 11, 15]. In order to generalize such an

approach to viscoelastic flows, a new software has been developed here, with new and more efficient data structures.

5.1 Sphere problem

For the first problem, we use the Maxwell-B fluid and we impose no-slip conditions along the sphere, falling at a constant velocity V . The radius of the sphere is half the radius of the cylinder and our calculation domain extends from $-15R$ to $30R$, with the sphere centered at the origin. The drag correction factor is defined by the ratio between the drag D exerted on the sphere and the drag D^0 exerted by a creeping Newtonian flow on a sphere in an infinite space, given by $D^0 = 6\pi\eta_V VR$.

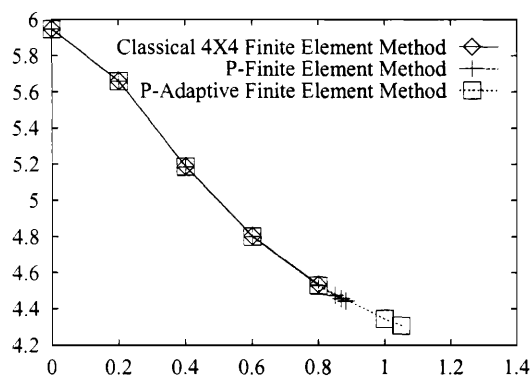


Figure 1: Sphere problem ($Re=0$), Maxwell-B fluid. Drag correction factor vs We number.

We compare the drag correction factors obtained at increasing We with several low- and high-order finite elements. These results are reported on Figure 1. With a classical low-order method (taken from [7]), numerical inaccuracies developed during the calculations prevent the continuation scheme to reach We numbers larger than 0.8. The stresses are interpolated with 4×4 linear subelements, while velocities and pressure are, respectively, biquadratic and bilinear. A very fine mesh is used with 510 elements and 38644 degrees of freedom.

A p -finite element method with 3 times less degrees of freedom, allow us to reach $We = 0.9$. The order of approximation for stresses, velocities and pressure are set, respectively, to 6,5 and 4 throughout the mesh.

Using a purely p -adaptive finite element method, local enrichments of the stress field up to order 7 bring the critical We number to 1.1. Note that less than 5% extra degrees of freedom were needed for this computation, if compared with the p -method.

In this smooth case, it is not optimal to apply local h -refinements. Global or local p -enrichments lead to impressive reductions of the number of degrees of freedom and to an increased robustness of the algorithm.

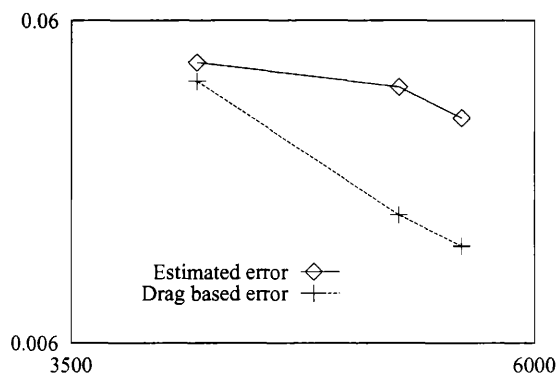


Figure 2: Sphere problem ($Re=0$), Maxwell-B fluid. Error index vs Number of degrees of freedom.

Using the estimation technique described above, we compute the *a posteriori* error estimates obtained during a pure p -adaptive process. Although no analytical proof is available for this estimator, comparisons can be made with a reference solution to validate the proposed procedure. It can be pointed out that the error estimator provides a similar evolution with mesh enrichments, as obtained if we compare the calculated drag with a reference value (given in [7]). The two curves are plotted on Figure 2. Such *drag based* error estimator is in fact unavailable in practical problems, where we do not have any reference.

5.2 Axisymmetric contraction problem

The second problem considered is the steady motion of a viscoelastic fluid through an abrupt 4:1 contraction. We impose $\mathbf{v} = \hat{\mathbf{v}}$ and $\boldsymbol{\tau}_V = \hat{\boldsymbol{\tau}}_V$ on $\partial\Omega_{Inflow}$, assuming that these fields are fully developed. We suppose that the fluid sticks to the wall and we impose zero normal velocity and zero tangential force along the axis of symmetry. Only velocities are imposed at the exit section, which is taken long enough to insure a fully developed profile. This profile is chosen to achieve global mass conservation in Ω . The lengths of the entry and exit sections are equal to 20 downstream radii.

In the particular case of an Oldroyd-B fluid ($F = 0$, $\eta_V/(\eta_N + \eta_V) = 0.875$), the particular form of Equation (2) may lead to non-integrable extra-stresses at the reentrant corner. We compare several adaptive strategies in order to

monitor the behaviour of the solution in the presence of a singularity.

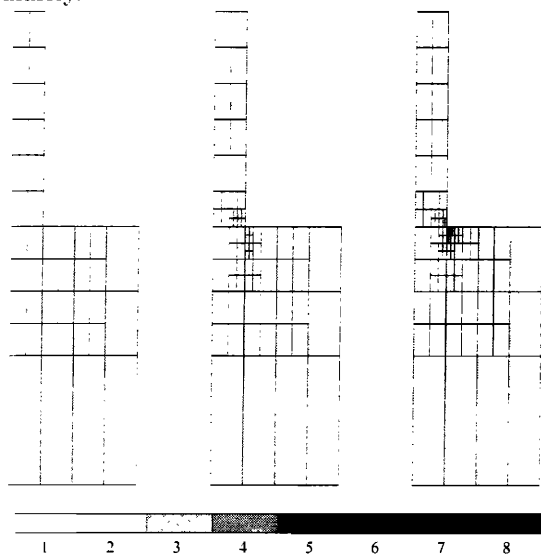


Figure 3: Abrupt 4:1 contraction ($Re=0, We=2$), Oldroyd-B fluid. Closeup view of the meshes.

Pure h -refinements As in classical finite element methods, convergence is obtained by splitting elements into smaller ones. These refinements occur mainly at the vicinity of the singularity (see Figure 3), which lead to the convergence curve plotted in Figure 6.

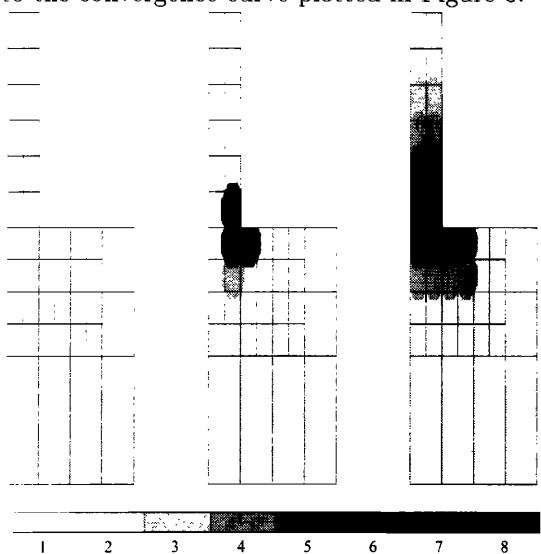


Figure 4: 4:1 Contraction ($Re=0, We=2$), Oldroyd-B fluid. Closeup view of the meshes.

Pure p -enrichments We know from approximation theory that p -enrichments only reduce the error with an algebraic rate of convergence in presence of a singularity.

This is well observed for this viscoelastic problem and the convergence rate of this p -finite element method is the same as the rate obtained with the classical h -method (see Figure 6). The three successive meshes used are shown in Figure 4, where shaded elements reflect a non-uniform p -distribution.

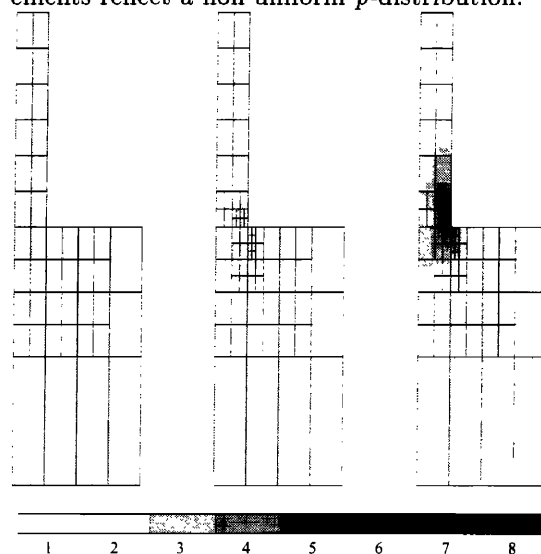


Figure 5: 4:1 Contraction ($Re=0, We=2$), Oldroyd-B fluid. Closeup view of the meshes.

Mixed h - and p -refinements In our hp -adaptivity, the first step consists of pure h -refinements. This h -refined mesh is then modified by pure p -refinements, leading to a higher global convergence rate of the method (as shown in Figure 6). Figure 5 presents the different meshes used in this approach.

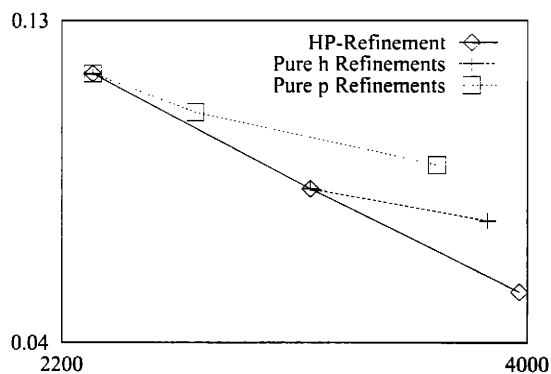


Figure 6: 4:1 Contraction ($Re=0, We=2$), Oldroyd-B fluid. Error index vs Number of degrees of freedom.

Now using a MUCM model, Equation (3) leads to a

Newtonian behaviour of the fluid in singularity areas. The stresses remain square integrable and pure p -refinements give the highest rate of convergence, as shown in Figure 7.

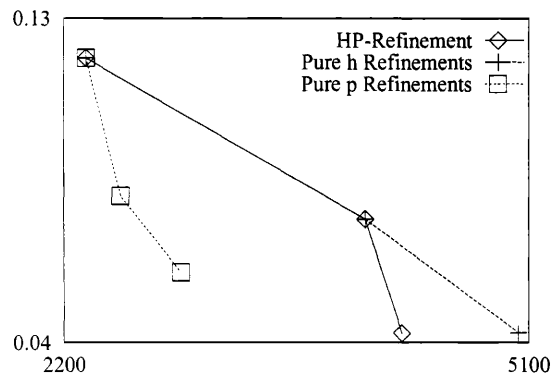


Figure 7: 4:1 contraction ($Re=0, We=6$), MUCM fluid. Error index vs Number of degrees of freedom.

6 Conclusions

An hp -adaptive finite element method has been proposed to solve viscoelastic flow problems in complex geometries. An *a posteriori* error estimation procedure has been set up, generalizing rigorous results of Oden et al. for Stokes and Navier-Stokes equations. Earlier experiments which illustrated the validity of the estimator on the 4:1 contraction have been confirmed on the sphere problem, taking the drag correction factor as relevant parameter.

Numerical results obtained on both test problems show how the domain geometry and the form of the constitutive equations affect the rate of convergence. This allows us to select well-suited adaptive strategies and to save many degrees of freedom. The CPU time required to achieve a target error is therefore significantly reduced.

7 Acknowledgements

This paper presents research results of the Belgian Programme on Interuniversity Poles of Attraction, initiated by the Belgian State, Prime Minister's Office for Science, Technology and Culture. The scientific responsibility rests with its authors.

References

- [1] M. Ainsworth and J.T. Oden. A procedure for a posteriori error estimation for h-p finite element methods. *Computer Methods in Applied Mechanics and Engineering*, 101:73–96, 1992.
- [2] M. Ainsworth and J.T. Oden. A unified approach to a posteriori error estimation using element residual methods. *Numer. Math.*, 54, 1993.
- [3] M.R. Apelian, R.C. Armstrong, and R.A. Brown. Impact of the constitutive equation and singularity on the calculation of stick-slip flow : the modified upper convected maxwell model. *Journal of Non Newtonian Fluid Mechanics*, 27:299–321, 1988.
- [4] A.N. Beris, R.C. Armstrong, and R.A. Brown. Spectral/finite element calculations of the flow of a maxwell fluid between eccentric rotating cylinders. *Journal of Non Newtonian Fluid Mechanics*, 22:129–167, 1987.
- [5] P.J. Coates, R.C. Armstrong, and R.A. Brown. Calculation of steady-state viscoelastic flow through axisymmetric contractions with the eeme formulation. *Journal of Non Newtonian Fluid Mechanics*, 42:141–188, 1992.
- [6] M. J. Crochet. Numerical simulation of viscoelastic flow : a review. *Rubber Chemistry and Technology*, 62:426–455, July 1989.
- [7] F. Debae, V. Legat, and M.J. Crochet. Practical evaluation of four mixed finite element methods for viscoelastic flow. *Journal of Rheology*, 38(2):421–442, 1994.
- [8] L. Demkowicz, J.T. Oden, W. Rachowicz, and O. Hardy. Toward an universal h-p adaptive finite element strategy, part I. constrained approximation and data structure. *Computer Methods in Applied Mechanics and Engineering*, 77:79–112, 1989.
- [9] V. Van Kemenade and M.O. Deville. Application of spectral elements to viscoelastic creeping flows. *Journal of Non-Newtonian Fluid Mechanics*, 51, 1994.
- [10] V. Legat and J.T. Oden. An adaptive h-p finite element method for incompressible free surface flows of generalized newtonian fluids. *Zeitschrift fur Angewandte Mathematik und Physik*, 46:643–678, 1995.
- [11] J.T. Oden, L. Demkowicz, W. Rachowicz, and T.A. Westermann. Toward an universal h-p adaptive finite

element strategy, part II. a posteriori error estimation. *Computer Methods in Applied Mechanics and Engineering*, 77:113–180, 1989.

- [12] J.T. Oden, A. Patra, and Y. Feng. An *hp*-adaptive strategy. In A.K. Noor, editor, *Adaptive, Multilevel and Hierarchical Computational Strategies*, volume 157 of *AMD*, pages 23–46. ASME, 1992.
- [13] J.T. Oden, W. Wu, and M. Ainsworth. An a posteriori error estimate for finite element approximations of the navier-stokes equations. *Computer Methods in Applied Mechanics and Engineering*, 14:23–54, 1994.
- [14] J.T. Oden, W. Wu, and V. Legat. An *hp* adaptive strategy for finite element approximations of the navier-stokes equations. *Int. Journ. for Numer. Methods in Fluids*, 20:831–851, April/May 1995.
- [15] W. Rachowicz, J.T. Oden, and L. Demkowicz. Toward an universal h-p adaptive finite element strategy, part III. design of h-p meshes. *Computer Methods in Applied Mechanics and Engineering*, 77:181–212, 1989.
- [16] A. Souvaliotis and A.N. Beris. Application of domain decomposition spectral collocation methods for viscoelastic flows through model porous media. *Journal of Rheology*, 36:1417–1453, 1992.
- [17] K.K. Talwar and B. Khomami. Application of higher order finite element methods for viscoelastic flows in porous media. *Journal of Rheology*, 36:1377–1416, 1992.
- [18] V. Warichet and V. Legat. An adaptive h-p finite element method for viscoelastic flows simulations. In *Proc. 2nd European Computational Fluid Dynamics Conference*, pages 181–187, September 1994.

